Physical circulation in the coastal zone of a large lake controls the benthic biological distribution.

Lakshika Girihagama[1*], E. Todd Howell[2], Jingzhi Li[1], and Mathew G. Wells[1].

[1] Department of Physical and Environmental Sciences, University of Toronto Scarborough, Toronto, Ontario, Canada.

[2] Environmental Monitoring and Reporting Branch, Ontario Ministry of Environment, Conservation and Parks, Toronto, Ontario, Canada.

[*]Corresponding author: Lakshika Girihagama (lakshika.rwrh@utoronto.ca)

Key Points:

- Conductivity gradients across the coastal zone of Eastern Georgian Bay (EGB) of Lake Huron limits the dreissenid mussel distribution.
- A circulation reminiscent of a partially mixed estuary in the fragmented archipelago controls the chemical and biological distributions.
- The seasonal character of solute gradient resulting from mixing in the coastal zone explains the spatial distribution of invasive mussels.

Abstract

There are gradients of conductivity and major ions in the coastal zone of the Eastern Georgian Bay of Lake Huron that appear to limit the spatial distribution of invasive dreissenid mussels. Rivers flowing into Georgian Bay from the Canadian Shield are relatively low in conductivity compared to the main body of Lake Huron, and so there is an observed gradient of solutes near the river mouths. The field observations show a strong positive correlation between conductivity and calcium concentration. Thus, we use conductivity to infer the solute concentrations required for the successful growth of dreissenid mussels. We observe most mussels in regions where specific conductivities were greater than 140 μS/cm. We use field observations to examine how the low calcium river water mixes within the coastal zone, which sets solute gradients that determine mussel distribution. When river flows are low, there is only a weak solute gradient across the coastal zone, implying an intrusion of open bay waters into the shallow embayments that is favourable for the growth of mussels. In contrast, when river flows are as much as 10 times higher, there is a strong solute gradient that extends further towards the lake, and the low calcium appears to inhibit and limit the growth of dreissenid mussels. Thus, the seasonal character of solute gradients helps describe the spatial distribution of dreissenid mussels and helps explain the localized absence of a species that is otherwise prevalent in much of the Laurentian Great Lakes.

1 Introduction

How physical water circulation patterns control species distribution in coastal aquatic systems remains a central question for aquatic ecologists. This is the case for the eastern coastline of Georgian Bay of Lake Huron where the abundance of invasive dreissenid mussels is low compared to the main body of the Lake Huron – Michigan system. It appears that the coastal solute gradients influence the distribution of these destructive invasive species here. In the Laurentian Great Lakes, dreissenid mussels consisting of zebra (*Dreissena polymorpha*) and quagga mussels (*Dreissena bugensis*) are now ubiquitous, after having first been identified in 1988 and 1989, respectively (Vanderploeg et al., 2002). Their distribution is broad, ranging from deep offshore waters to nearshore areas due to their ability to utilize both soft substrates and hard substrates in more energetic coastal zones (Hecky et al., 2004). Most importantly they have led to a fundamental shift in the food webs and ecosystems of the Great Lakes. For instance, the occurrence of dreissend mussels affects water quality (Hecky et al., 2004; Higgins et al., 2008; Higgins and Zanden, 2010; Howell et al., 1996), species diversity (Botts et al. 1996; Nalepa, 2010; Pothoven et al., 2001; Strayer et al., 2004), and inter-dependent anthropogenic effects on eutrophication problems such as blooms of benthic algae (Higgins et al., 2012). Although dreissenid mussels have wide environmental tolerances, they are not uniformly distributed or abundant around the Great Lakes, and for instance have the highest densities in Lake Erie (Mackie, 2004) and are largely absent from Lake Superior (Grigorovich et al., 2003). This is in part due to the restricted range of major ion chemistry under which the mussels flourish. Georgian Bay is part of Lake Huron and hence joined with Lake Michigan, which together functions hydrologically as a single lake of area 117,585 km². In all of this vast lake, eastern Georgian Bay has some of the softest water discharges from rivers, resulting in variability in major ion concentrations over ranges expected to affect mussel physiology. To predict how dreissenid mussels impact the aquatic ecosystem in these areas, it is useful to understand how nearshore lake circulation may structure chemical gradients that shape the species distribution.

Calcium is a key element for metabolic function and shell growth of mussels and hence determines if shells can form (Whittier et al., 2008; Jones and Ricciardi, 2005; McMahon, 1996). The lack of dreissenid mussels in much of Lake Superior and many smaller lakes on the Canadian Shield is believed due to the softness of the water where calcium concentrations are ≤12 mg/L (Grigorovich et al. 2003). In Lake Erie, on the other hand, mussels are abundant with an average calcium level of 38 mg/L (Mackie, 2004). Jones and Ricciardi (2005) found zebra mussels and quagga mussels absent below 8 mg/L and 12 mg/L of calcium, respectively, among sites along the St. Lawrence River. Based on laboratory studies, Davis et al. (2015) suggested that water bodies with 12-15 mg/L of calcium were at risk of invasion by quagga mussels. Whittier et al. (2008) used surface calcium concentrations data from 3000 rivers and streams in the United States to predict the distribution of dreissenid mussels. In their study, risk of occurrence based on calcium concentrations were very low (< 12 mg/L), low (12 – 20 mg/L), moderate (20 – 28 mg/L), and high (> 28 mg/L). These studies provide guidance on critical calcium concentrations for dreissenid mussels growth, however, knowledge of how lake circulation influences the spatial distribution of calcium is also needed to infer dreissenid mussel distribution in dynamic nearshore regions.

In contrast to most of the Great Lakes, which have fairly homogenous coastlines, the shore of eastern Georgian Bay (EGB) is complex consisting of an archipelago of 30,000 islands extending over 150 km of coastline. The archipelago ranges from 5 to 20 km wide resulting in broad transition zones from river-like conditions to the open lake. The local geology is heavily influenced by the past glaciations, consisting of a heterogeneous coastline with granitic and sedimentary rocks from the Precambrian Period (Sly and Munawar, 1988). There have been few studies of coastal circulation in EGB, except as part of the large-scale hydrodynamics of Lake Huron (Harrington, 1895; Csanady, 1968; Bennett, 1988; Sheng and Rao, 2006). In contrast to many more linear coastlines of the Great Lakes, the transport of solutes cannot be understood in terms of a coastal boundary layer (Rao and Schwab, 2007), rather it is more useful to consider the coastline as a sequence of river mouths that mix through an archipelago. Continuous exchange (net volume transport) and mixing (dispersion) of low conductivity river waters with high conductivity open bay waters generate a mixing zone. This results in downstream solute gradients reminiscent of circulation in estuaries.

Generally, EGB is thought to have some of the best water quality in the combined Lake Huron-Michigan, but there has been little study in EGB of the occurrence of dreissenid mussels along the coastline. Surveys by National Oceanic and Atmospheric Administration (NOAA) indicate a low to moderate abundance of dreissenid mussels in the offshore waters of Georgian Bay (Nalepa et al., 2018), however, the contrasting benthic habitat and water quality between the offshore and the coastline of EGB make it difficult to infer the inshore distribution of mussels from offshore data. Increased mussel levels in offshore regions have been linked to food-web changes whereby nutrients levels drop and filter–feeding by mussels means nutrients are cycled in nearshore with resulting increases in benthic algae (Hecky et al., 2004). The invasion of Lake Huron by dreissenid mussels in the last 30 years has corresponded with the ongoing oligotrophication of the lake, resulting in phosphorus levels indicative of ultra-oligotrophic conditions (Nalepa et al., 2007; Barton et al., 2013). Lake Huron has not yet seen a proliferation of benthic algae and the resulting shoreline fouling to the nearshore ecosystem analogous to those reported for the lower Great Lakes (except in Saginaw Bay, e.g., Budd et al., 2001; Nalepa and Fahnenstiel, 1995; Johengen et al., 1995). However recent monitoring in southeastern coastal zone of Lake Huron has also detected striking changes in the nearshore ecosystem, such as the expansion

of benthic algae (Barton et al., 2013; Howell, 2004) and lower than expected water column phosphorus levels (Howell et al., 2014).

Knowledge of the distribution of mussels in EGB is needed to anticipate the ecological trajectory of this high-quality ecosystem. Studies elsewhere in Lake Huron, the Great Lakes, and more broadly which have examined the pre- to post- dreissenid transition predict a wide range of environmental changes broadly described by the concepts of benthification and offshore-oligotrophication, however, in the case of EGB the uncertainty of whether the river loading of soft water to the coastline will mitigate these outcomes by limitation of mussel abundance is not known. The mixing of rivers in the coastal zone of EGB potentially shapes physiochemical gradients that influence the distribution of dreissenid mussels over the coastline given the characteristic mixing of relatively soft waters loaded from granitic tributaries into the moderately hard offshore waters of Georgian Bay. Seasonal gradients in calcium across the coastline are likely a result of the varying discharge volumes of low-calcium water from rivers and the variable mixing of offshore waters over the coastline (Figure 1) and thus, creating limited calcium levels (threshold levels) for successful colonization of these mussels. The setting of water quality gradients by complex hydrodynamics in nearshore regions of EGB has been previously demonstrated in terms of nutrient-related features in Severn Sound (Sherman et al., 2018) and Sturgeon Bay (Campbell and Chow-Fraser, 2018) but limited to highly localized conditions.

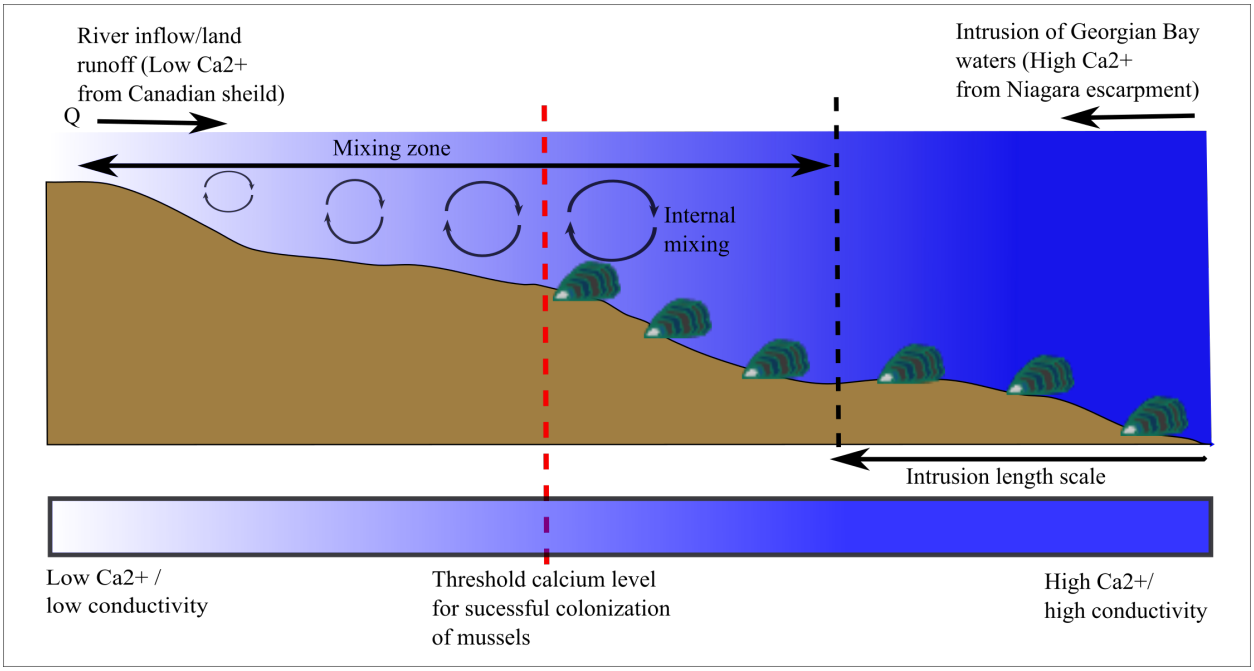

Figure 1. Schematic of the main physical processes setting the downstream solute gradient in the coastal zone of eastern Georgian Bay. High conductivity (calcium) waters from Georgian Bay mixes with the low conductivity freshwater from the Canadian Shield. The resulting horizontal mixing generates a mixing zone where the threshold calcium levels for successful colonization of mussels are created. The intrusion length scale is defined as the distance over which the landward intrusion of high conductivity Georgian Bay occurs (Reader may refer to section 4 for full details of the definition of intrusion length scale).

In this study, we use field observations to address the question of how physical hydrological processes, specifically along-stream mixing of fresh river water, influences the

biological distributions within coastal zones of a large lake. Specifically, we aim to answer whether observed solute gradients along two different river systems flowing into a large lake can explain the spatial distribution of dreissenid mussels. We study these processes in Eastern Georgian Bay, as there are strong gradients in calcium between the river mouths and offshore waters of the bay. The resulting solute gradients are due to the changes in surrounding geology from the carbonate-rich Niagara escarpment on the south-western shores of the bay to the granitic landscapes of the Canadian Shield on the north-eastern side of the bay. We use observations from two river systems with different hydrology to explore the influence of freshwater flux on the solute gradients, and the resulting dreissenid mussel distribution.

2 Materials and Methods

2.1 Study area

Georgian Bay, considered isostatic with Lake Huron, has a surface area of 15,111 km² and a mean depth of 44 m. It is separated from the main body of Lake Huron by a 20 km-wide channel between Manitoulin Island and the Bruce peninsula (45.4062° N, 81.1132° W) and is connected to the outflow of Lake Superior by the North Channel (Bennett, 1988; Sly and Munawar, 1988) (Figure 2 a, b). A defining feature of Georgian Bay is a fragmented archipelago of islands and bays along its eastern coastline abutting the longer north-south axis of the roughly rectangular basin of the lake measuring 75 km by 175 km (Bennett, 1988). The bedrock geology of Georgian Bay is shaped by past glaciation. The eastern coastline consists of granitic and sedimentary rocks from the Precambrian Period and the main basin contains mid-Silurian dolomite (Sly and Munawar, 1988). Seasonal stratification in the offshore of Georgian Bay is limited to upper 30 m (Sheng and Rao, 2006). The thermocline forms in July at depths of 15-30 m while temperatures below 45-60 m remain near 4 ^{0}C (Berst and Spangler, 1973). The general surface water circulation in Georgian Bay is cyclonic but reverses occasionally with the reversed winds (Sly and Munawar, 1988; Sheng and Rao, 2006). A summary of the physical limnology of Georgian Bay can found in Bennett (1988).

The field studies examining the distribution of dreissenid mussels in EGB were made along 100 km of coastline from Severn Sound to Shawanaga Inlet. The detailed examination of water circulation and solute gradients over the coastline was limited to within the Shawanaga Inlet (SI) and Moon River (MR) regions (Figure 2c, d). Shawanaga Inlet is an elongated channel aligned in the NE-SW direction with a length of 13 km and with a mean depth of 5.8 m. In contrast, Moon River is a wide basin (~15 km) with a cluster of islands with maximum and mean depths of 30 m and 7.6 m, respectively.

2.2 Physical and chemical field measurements

Spatial measurements of solute distribution and thermal stratification in SI and MR areas were collected in 2015 to identify mixing gradients along the land to lakes axes of the coastal zone. The coastal zone in the archipelago as operationally defined here is the portion of the shoreline waters connected to the open lake extending offshore to past the furthest reef or island. These point-in-time vessel surveys conducted by the Ontario Ministry of Environment, Conservation and

Parks (MECP) were complemented by seasonal monitoring of lake currents, temperature, and conductivity at discrete moorings.

During vessel surveys, a range of near-surface field measurements was collected over pre-defined survey tracks (the solid blue line in Figure 2c, d). The survey tracks, extending over 50-100 km, ranged from the exposed offshore to the limits of navigable depth within embayments. The SI and MI study polygons are approximately 20x30 km^2 and 14x18 km^2, respectively. Surveys were conducted twice; SI (June 16-17, 2015 and Sept 21-23, 2015) and MR (June 23-25, 2015 and Sept 28-30, 2015). The vessel surveys used sensors connected to a flow-through manifold on the deck of the vessel drawing from 1.5 m below the surface to provide near-continuous measurements at approximately 5 m intervals. An RBR XR-620 probe measured temperature and conductivity with an accuracy of ± 0.002 °C and ± 0.003 mS/cm, respectively. Measurements were updated by the data acquisition software at a frequency of approximately 3 Hz which was then sampled at 5 m intervals. Discrete samples of water were collected for lab-based analysis of calcium at points distributed over the survey track. Calcium concentrations in whole water samples were analyzed by Inductively Coupled Plasma Optical Emission Spectrometry (ICP-OES) at the Ontario Ministry of the Environment, Conservation and Parks (MECP) labs in Toronto using Laboratory Services Branch method E3497. The instrument setup uses an APEX E desolvation system. The MDL for calcium is 0.00465 mg/L.

Point-in-time temperature values are used to calculate the corresponding point-in-time conductivity measurements to specific conductivity by adjusting conductivity by 1.9% per degree upward below 25 ^{0}C and downward for each degree above 25 ^{0}C. The majority of ion equivalents in solution over the high conductivity range consisted of Ca^{2+} and HCO^{3-} ions, however, at the lower range of conductivity values, Na^+ and Cl^- ions contribute ion equivalents approached that of Ca^{2+} and HCO^{3-} ions (data not shown). With few exceptions, Ca^{2+} and HCO^{3-} ions continued to be the largest contributor to ion equivalents in solution. The same method of inferring specific conductivity was used across the full conductivity range of samples.

Acoustic Doppler Current Profilers (ADCP), conductivity probes, and temperature strings were deployed from April to November of 2015 over the SI and MI areas to measure physical features of coastline (the red circles given in Figure 2c, d; see Table S1 for the detailed list of instruments and measured parameters). At every 30 minutes, the water column temperature was recorded with HOBO Tidbit loggers attached to a vertical string with a 1 m depth interval. Upward–looking ADCP units (RDI 600 kHz workhorse) with a 1 m bin size measured current speeds and direction at a sampling rate of 30 minutes. Conductivity sensors (anti-fouling ALEC Electronics Compact-CLW) deployed at mixing points between the inshore and offshore lake provided information on temporal changes in conductivity gradients. All conductivity data are reported as specific conductivity at a sampling rate of 30 minutes.

Our two study sites, SI and MR mainly receive freshwater from two rivers, namely, the Shawanaga river and the Moon river. Shawanaga river is 60 km long with a drainage area of 235 km^2. Moon river is 261 km long with a drainage area of 4790 km^2. The discharge of Moon river is determined from the water gauge (Gauge ID: 02EB011; Data source: Environment Canada water office) that is located close to Georgian Bay. There were no active down river gauges for Shawanaga River in 2015. Thus, Shawanaga River discharge (Q_1) for 2015 was estimated from the nearby Magnetawan watershed that has a similar drainage area (A_2) with a discharge of Q_2

whereby $Q_1/A_1 = Q_2/A_2$ (Morrison and Smith, 2001); where A_1 is the watershed area of Shawanaga river. Based on river gauges available, we averaged discharge from the nearby gauge stations North Magnetawan River near Burk's Falls (Gauge ID: 02EA005; drainage area: 329 km^2) and North Magnetawan River above Pickerel Lake (Gauge ID: 02EA010; drainage area: 155 km^2) to calculate approximate river discharge for Shawanaga river.

2.3 Benthic biological field measurements

The spatial distribution of dreissenid mussels along EGB coastline was determined from diver collected and Ponar grab benthic samples. These were collected in SI, MR, Parry Sound, Go Home Bay, and Severn Sound areas (Figure 2e). Divers collected benthic samples on hard substrate at 43 sites on July 8 to 23 and September 8 to 10 in 2014. At these sites, dreissenid mussels were collected from three randomly placed quadrats (0.15 m^2) and used to estimate mussel abundance. Sites ranged from 3 to 20 m in depth. Samples were frozen after collection and later freeze-dried for counting. In 2015, using a 9-inch Ponar grab, benthic samples on soft substrate were collected at 45 sites from August 6 to 16. The numbers of dreissenid mussels in triplicate samples preserved in formalin and filtered with 600 μm mesh were determined at each site. The geographical distribution of sample sites is shown in Figure 2e. Water column profiles of conductivity and pH were collected at the same time of benthic sampling using AMT profiling sonde. Water-column averages of data are reported subsequently.

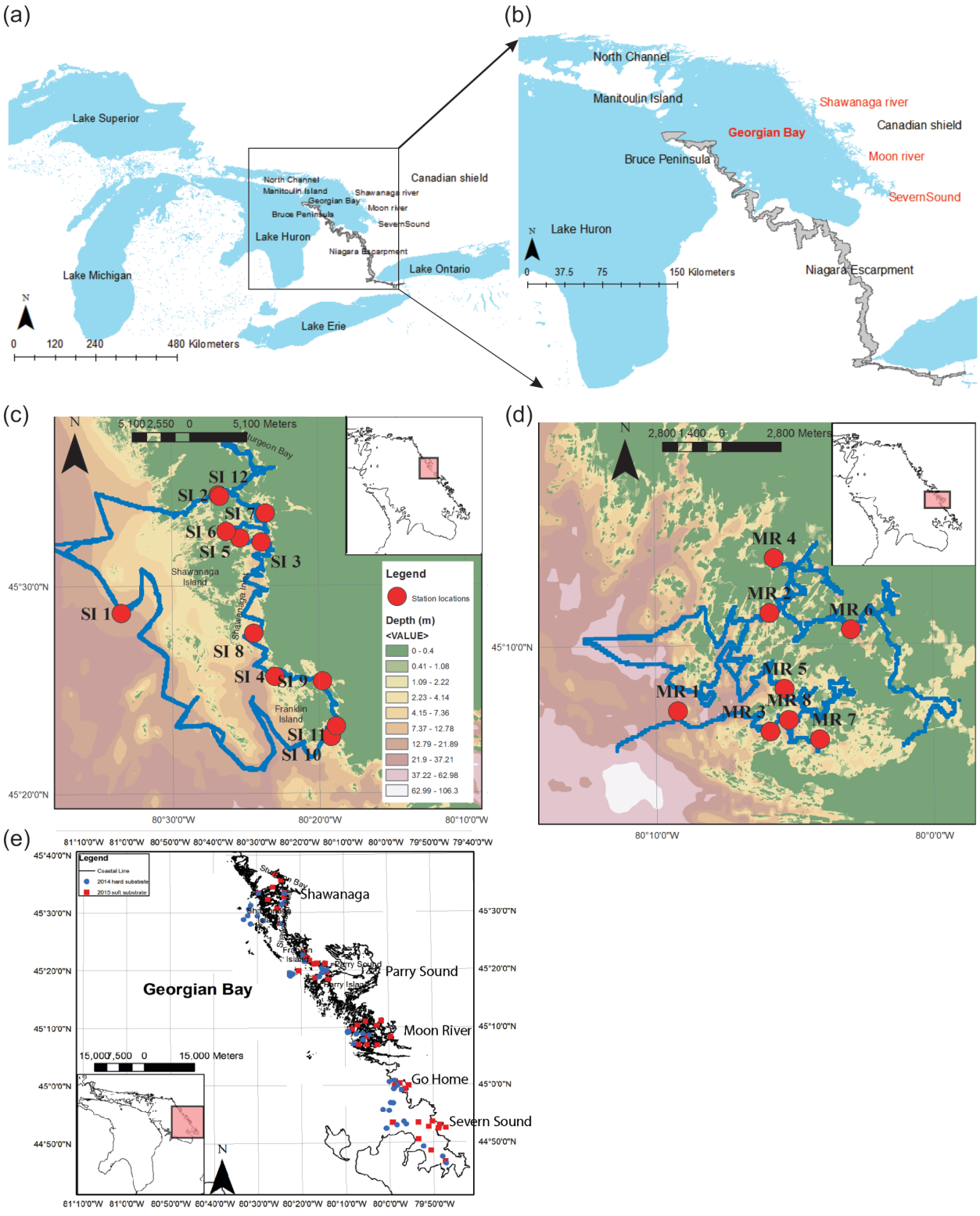

Figure 2. (a) Geographical position of Georgian Bay compared to the rest of the Great Lakes. (b). Exaggerated view of the Georgian Bay. (c). The detailed locations and routes for physical and water quality field data collection campaigns for (c) SI and (d) MR are shown with their

corresponding bathymetry. The 2015 survey track for MR and SI is given as the blue solid line. The two survey tracks are completed for each study area (MR and SI) in June and in September. The blue circles denote the geographical locations of the moorings in (c) SI and (d) MR. Data is recorded continuously every 30 minutes from May-Nov 2015. The length of the SI is 13 km. The mean depth is 5.8 m. The length of MR is ~15 km with a mean depth of 7.6 m. Data is from ESRI Great Lakes Bathymetry Contours. (e) Geographical locations of benthic sampling sites in 2014 and 2015. The red circles denote the 43 sites where samples were collected on the hard substrate by divers in 2014. The red squares denote the 45 samples that were collected on the soft substrate in 2015 using a Ponar grab. The names of the sample locations in EGB are SI, Parry Sound, Go Home Bay, MR, and Severn Sound.

2.4 Physical data analysis describing advective and dispersive processes.

The distribution of solutes and hence the gradient across the coastal zone of EGB is governed by the transport and mixing of low solute river waters with the high solute waters of Georgian Bay. The transport (exchange) of solutes is twofold and is known as barotropic and baroclinic motions. The currents in barotropic motion are driven by the surface elevation gradient caused by wind forcing and river inflow. Baroclinic motion takes place when there is a vertical density gradient such as when high conductivity waters from the open bay flow landward along the bottom while relatively fresh surface water flows in opposite direction to the bottom landward flow. The time scales of these baroclinic or barotropic motions vary from hourly to seasonal. At a quasi-steady-state (motion averaged over the dominant period oscillation), the balance between the advection (volume transport) and dispersion (mixing) defines the mixing zone between river waters with open bay waters and how far upstream intrusions of lake water can flow into the archipelago. The length scale associated with this intrusion of lake water can be defined as a function of the horizontal dispersion coefficient ($\boldsymbol{K_x}$) and the net volume transport ($\boldsymbol{Q}$).

2.4.1 Decomposition of motion to barotropic and baroclinic motion

Empirical Orthogonal Function (EOF) analysis was used to decompose the patterns of the variability in the velocity field to identify the dominant modes of exchange processes (baroclinic and barotropic) and the magnitude of their contributions as a linear sum of modes. The method is widely used in oceanography (Kawamura, 1994; Kaihatu et al., 1998; Levitus, 2005; Casagrande et al., 2011). EOF analysis describes the spatial and temporal variability as orthogonal patterns or modes from eigenvalues and eigenvectors of the covariance matrix of each orthonormal basis generated by the measured data field. Eigenvalues resulting from EOF's modes are a measure of the percentage of the total variance of the measured data and ranked ordered by the magnitude of the variance of the patterns. For velocity, the variance in each orthonormal basis is defined as the energy, and eigenvalues are ranked ordered from high energy to low energy. In this analysis, EOF is performed on measured currents at open bay (SI1, SI8, and MR1) and near river mouths (SI6, and MR3) sites. Each EOF mode consists of a time-varying component known as the principal component (expansion coefficient) which gives the temporal variability of each EOF.

2.4.2 Dominant periods of motion

The velocity fluctuations in EGB vary on seasonal to hourly time scales. Fast Fourier Transform (FFT) of the depth-averaged velocity time series was used to extract the dominant

periods of total water column motion. In each dominant cycle, the system is in a quasi-steady state where high-frequency motions become null. Hence, the power spectrum is estimated by transferring the time domain to the frequency domain (Welch, 1967). The division of stationary data into segments is applied to acquire the modified periodogram for each segment (the uncorrelated estimates of the spectra). Before taking the average periodogram, a multiplication of each segment by a window function (Hanning) and 50% overlap of each segment was applied to reduce the variance.

2.4.3 Excursion length estimates for each forcing cycle

The appearance of Lagrangian drift-like motion in the Progressive Vector Diagram (PVD) is an approximate indicator for the downstream trajectory of a water parcel measured at a point location. Dispersion of solutes within the water column occurs along this trajectory. PVD can be used to estimate the average excursion length scale of the trajectory for each forcing cycle (Figure S10a-b).

2.4.4 Estimation of horizontal dispersion coefficient

A useful estimate of lateral mixing is given by the horizontal dispersion coefficient ($\boldsymbol{K_x}$). Although there are no estimates of dispersion coefficients for EGB, work in other parts of the Great Lakes suggests a wide range of values. There is a length scale dependence of ($\boldsymbol{K_x}$) Murthy (1976) showed that the ($\boldsymbol{K_x}$) value varies from 0.01 to 10 m^2s^{-1} for a length scale varying from 100 m to 15 km in the epilimnion in Lake Ontario. Csanady (1963) found the maximum diffusion coefficient was ~ 0.04 m^2s^{-1} for a length scale up to 1 km for the epilimnion of Lake Huron. Further, Rao and Murthy (2001) showed that ($\boldsymbol{K_x}$) is in the range of 0.02 m^2s^{-1} to 2.0 m^2s^{-1} in coastal zones of Lake Ontario during summer for length scales of 1-10 km. Rao et al. (2008) showed ($\boldsymbol{K_x}$) was in the general range of 0.2 m^2s^{-1} to 1.2 m^2s^{-1} in the central basin of Lake Erie.

The horizontal dispersion coefficient can be estimated from continuous measurements of horizontal currents at moorings-ADCPs (Schott and Quadfasel, 1979; Rao and Murthy, 2001; Rao and Murthy, 2008). The idea of determination of Lagrangian dispersion coefficient using moored currents is to transfer Eulerian fluctuations to Lagrangian variance (Taylor, 1922; Hay and Pasquill, 1959; Schott and Quadfasel, 1979; Rao and Murthy, 2001; Rao and Murthy, 2008). In stationary and homogenous fluctuating flow fields the Lagrangian velocity variance is equal to the Eulerian velocity variance ($\langle \boldsymbol{u'^2} \rangle$). The shape of the autocorrelation function of the Lagrangian velocity variance can be obtained by multiplying the autocorrelation function of Eulerian velocity fluctuations by a factor ($\boldsymbol{\beta > 1}$). Thus, the horizontal dispersion coefficient from Eulerian velocity is defined as $\boldsymbol{K_x = \beta \langle u'^2 \rangle T}$ such that, $\boldsymbol{T = \int_0^\infty R(\tau) d\tau}$ where $\boldsymbol{T}$ is the Eulerian integral time scale and $\boldsymbol{R(\tau)}$ is the autocorrelation function. Following this method, first, we removed the lowpass filtered (<24 h) signal from the horizontal currents to acquire the velocity variance and then calculated the autocorrelation function. Then we integrated the autocorrelation function until the first zero crossing to acquire the Eulerian integral time scale. It is important to note that the selection of $\boldsymbol{\beta}$ determines the accuracy of the predicted horizontal dispersion coefficient. However, due to the lack of Lagrangian observations in Georgian Bay to determine $\boldsymbol{\beta}$, we followed other studies from the Baltic Sea, Lake Ontario, and Lake Erie (Schott and Quadfasel, 1979; Rao and Murthy, 2001; Rao and Murthy, 2008) and we selected the $\boldsymbol{\beta = 1.4}$.

3 Data and Results

3.1 Benthic dreissenid mussel distribution

Low densities of dreissenid mussels (*D. polymorpha* and *D. bugensis*) were more broadly distributed on the open shores of the bay than the connected channels and embayments during benthic surveys in July and September 2014 and August 2015 (Figure 3). Both species were present at 42 of the 55 sites. The density of *D. bugensis* was higher than *D. polymorpha* at most sites with *D. polymorpha* contributing <50% of numbers at 46 of 52 sites with *D. polymorpha* present. Maximum density was less than 1000 individuals/m^2 in most areas except for Severn Sound where the maximum density was 4800 individuals /m^2 (Figure 3e). In 2015, mussels were found at only 8 of 43 soft-sediment sites at < 500 individuals /m^2 except for two sites in Severn Sound (Figure 3e). Severn Sound is a large embayment on the north-south boundary of southern EGB that separates the limestone from the granitic geology of the coastline. The area is more developed than other parts of EGB with a history of nutrient enrichment and more a productive trophic state. In general, the soft sediment sites were in depositional areas located further inshore than the sites with hard substrate which were more exposed to the open bay.

Mussels density on hard substrate was strongly correlated with conductivity (Figure 4a). Mussels were not found on either substrate type at sites with specific conductivity < 140 µS/cm except for two sites with < 15 individuals/m^2. Given this low abundance compared to other sites with mussels where water column specific conductivities were > 140 µS/cm, we infer that successful establishment of dreissenid mussel populations is minimal when the summer-measured specific conductivities are less than 140 µS/cm. Mussel abundance on hard substrate at specific conductivities >140 µS/cm is positively correlated with conductivity (R^2=0.37, p-value <0.0001). Mussels were not detected on soft substrate at specific conductivity < 158 µS/cm, however, abundance was not correlated with conductivity. Mussel abundance did not exceed 1000 individuals/m^2 at sites with conductivity less than 180 µS/cm. Field measured pH was unrelated to mussel abundance other than that range in abundance was wider at higher pH (Figure 4b).

Calcium concentration is strongly correlated with conductivity over the geographic range of the benthic sites and suggests that the relationship between conductivity and mussel abundance stems from the association between conductivity and calcium (Figure 4c). Calcium concentration can be predicted from conductivity (R^2=0.98, n=730) based on a spatially and seasonally wide dataset collected by MECP in 2015 and 2016 during the monitoring of water quality in EGB. The calcium concentration is low in discharge from the low conductivity rivers draining granite bedrock on the Canadian Shield. In contrast, the open waters of Georgian Bay have higher conductivity due to the calcareous geology in much of the shoreline and basin of Lake Huron. Disassociated carbonates account for much of the ionic content of the waters of Lake Huron. Dreissenid mussel distribution is strongly influenced by calcium concentrations (Whitteir et al., 2008). We infer a calcium concentration of 14.8 mg/L that corresponds to specific conductivity of 140 µS/cm (red dashed line in Figure 4c) as a threshold for successful colonization of dreissenid mussels in EGB based on summer-measured conductivity, a period when conductivity is anticipated to be at seasonal highs.

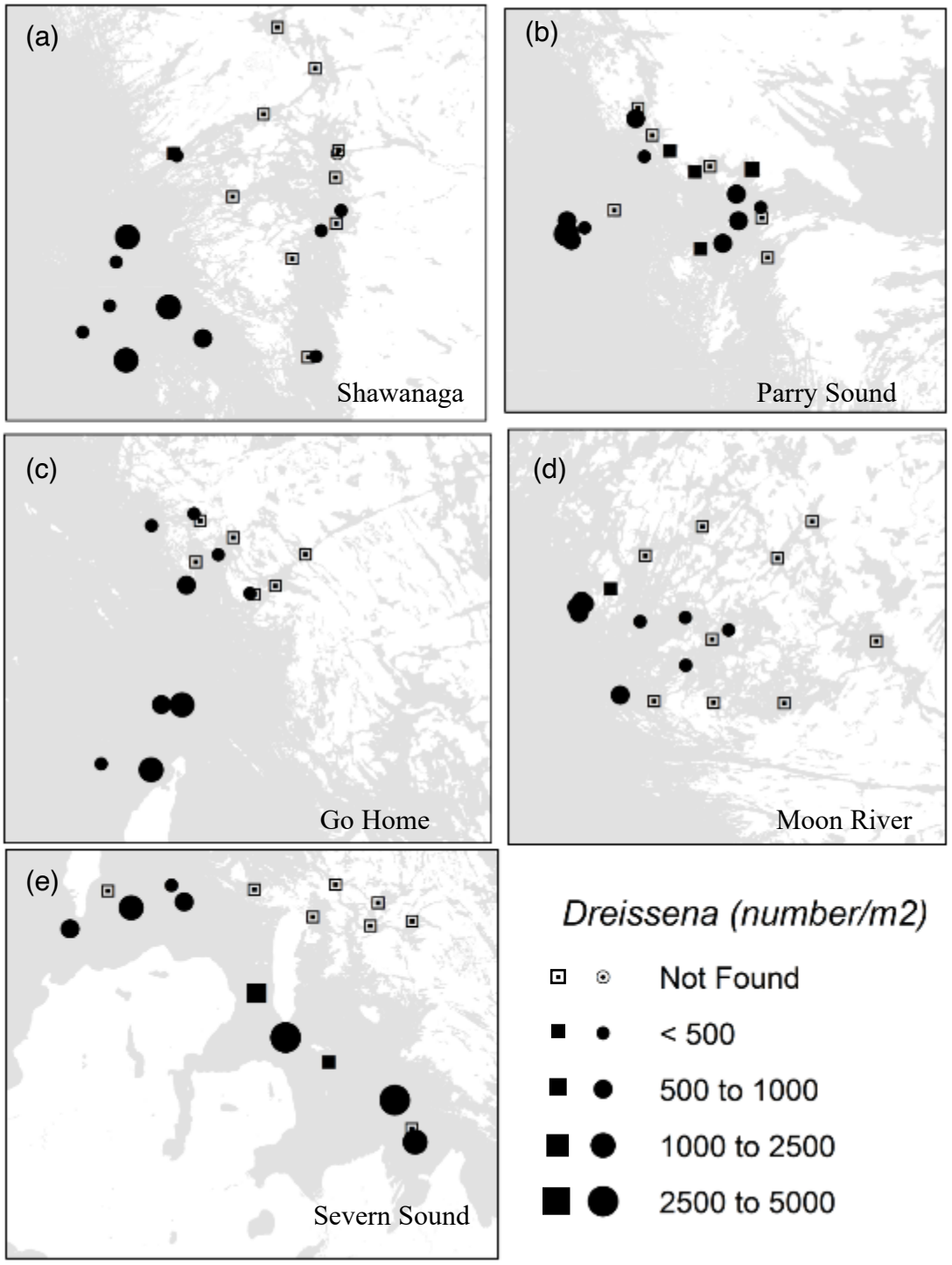

Figure 3. Numbers of dreissenid mussels in the nearshore of EGB. (a) SI (b) Parry Sound (c) Go Home Bay (d) MR and (e) Severn Sound. The circles and squares represent abundance on hard substrate in 2014 and soft substrate in 2015, respectively. The scaling of the size of the squares is the same as for circles shown in the figure legend.

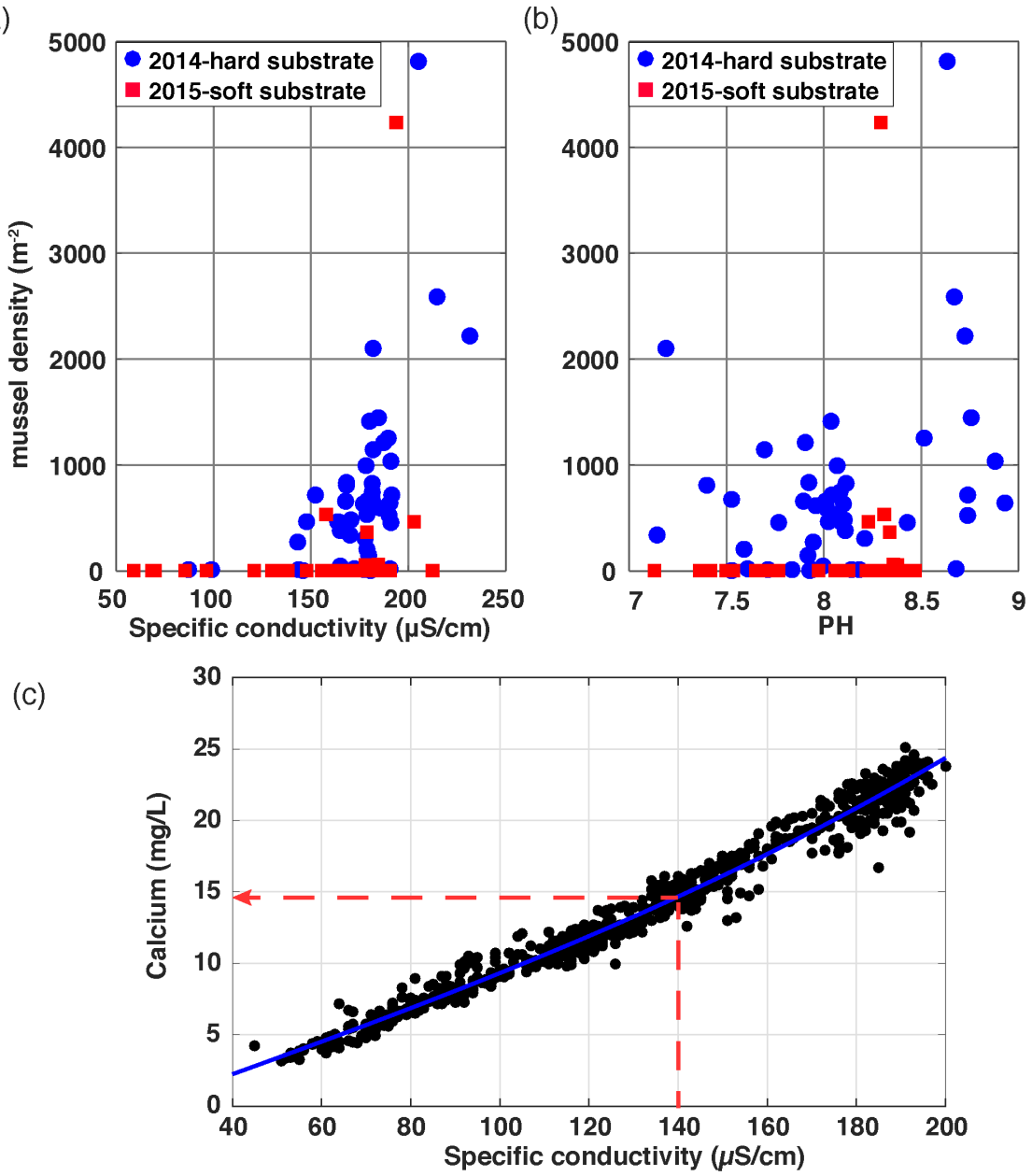

371

372 **Figure 4.** Mean number density of dreissenid mussels at sites plotted against (a) average water
373 column conductivity and (b) pH as measured at the time of benthic sampling. The circles and
374 squares indicate results for surveys on hard substrate in 2014 and soft substrate in 2015,
375 respectively. (c) The correlation between the Ca^{2+} concentration and the conductivity of collected
376 water samples in 2015 and 2016 by MECP monitoring of water quality in eastern Georgian Bay.
377 The line is a cubic fit to the data used to estimate expected calcium concentration at a given
378 conductivity. The curve is $\mathrm{Ca} = -2.26 + 0.11(\mathrm{conductivity}) - 0.00005(\mathrm{conductivity})^2 +$
379 $0.000007(\mathrm{conductivity})^3$ with conductivity in units of µS/cm; $R^2 = 0.98, n = 730$. The red

dashed line shows the dissolved calcium concentration of 14.8 mg/L at the threshold conductivity of 140 µS/cm.

3.2 Conductivity gradient across the coastal archipelago of EGB

Spatial surveys of water quality conducted in 2015 over SI and MR areas of EGB confirmed the expected conductivity and calcium gradients across the coastal zone (Figure 5). The lowest conductivity and calcium concentrations were observed at the river mouths and increased towards offshore. Conductivity was less variable in the open bay with specific conductivity of approximately 180 and 190 µS/cm at the time of the June and September 2015 surveys, respectively (Figure 5). The conductivity gradient in September surveys shows a significant mixing of open bay waters with the shallow embayments and hence a weaker solute gradient across the coastal zone and a large intrusion length scale of lake water into the embayments.

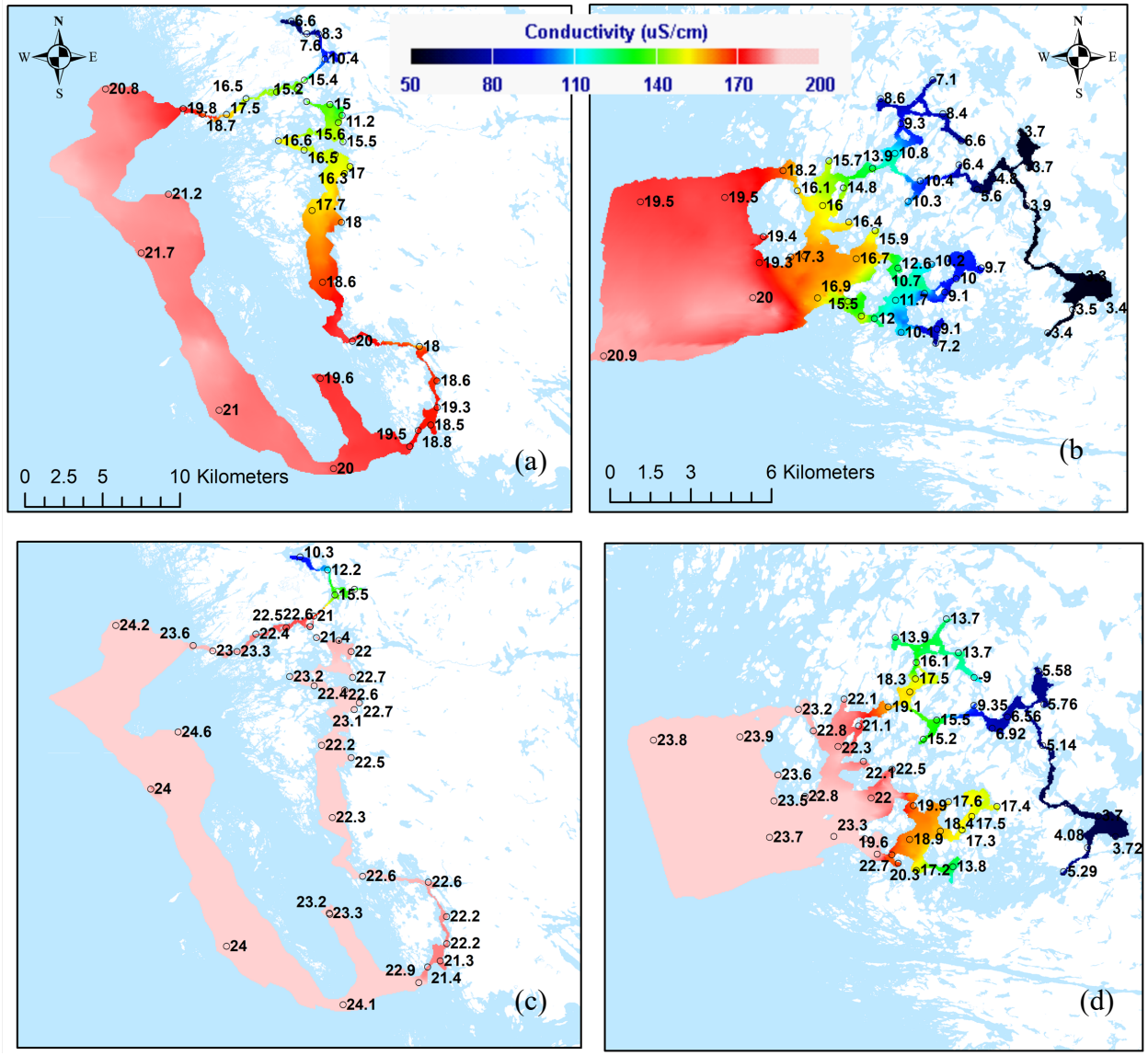

Figure 5. Spatial distribution of specific conductivity in (a) Shawanaga River region (SI) for June 16-17, 2015 (DOY 167-168), (b) Moon River region (MR) for June 21-23, 2015 (DOY 172-174),

394 (c) SI for September 21-23, 2015 (DOY 264-266), and (d) MR for September 28-30, 2015 (DOY
395 271-273). The numbers marked along with the symbol 'o' on the spatial maps of conductivity in
396 both regions denote the calcium concentration (mg/L) measured periodically along the survey
397 route.

398 Spatial gradients in conductivity were also observed at moorings located between the open
399 waters of Georgian Bay and river mouths (Figure 6). The locations of moorings MR1, MR2, and
400 MR6 and SI1, SI3, SI7, SI8, SI9, and SI12 are shown in Figure 2. Moon river MR1 is in open
401 waters, and MR6 furthest up channel, while for Shawanaga Inlet SI1 is in open waters, and SI7
402 furthest up channel. At these moorings, the specific conductivity was lower at inshore sensors
403 compared to those located at open waters sites. For example, on June 24 (DOY 175), the specific
404 conductivity close to the Moon River (mooring MR6) was ~60 µS/cm compared with mooring
405 MR1 located in the open water where conductivity was ~180 µS/cm. Specific conductivity at the
406 open water sites (MR1 and SI1) stayed at ~180 µS/cm over the measurements period contrasting
407 with sites placed close to river mouths which varied seasonally. For example, SI7 showing a
408 gradual increase of conductivity from ~80 µS/cm from May (~DOY 120) to ~180 µS/cm by Mid
409 -July (~DOY 200).

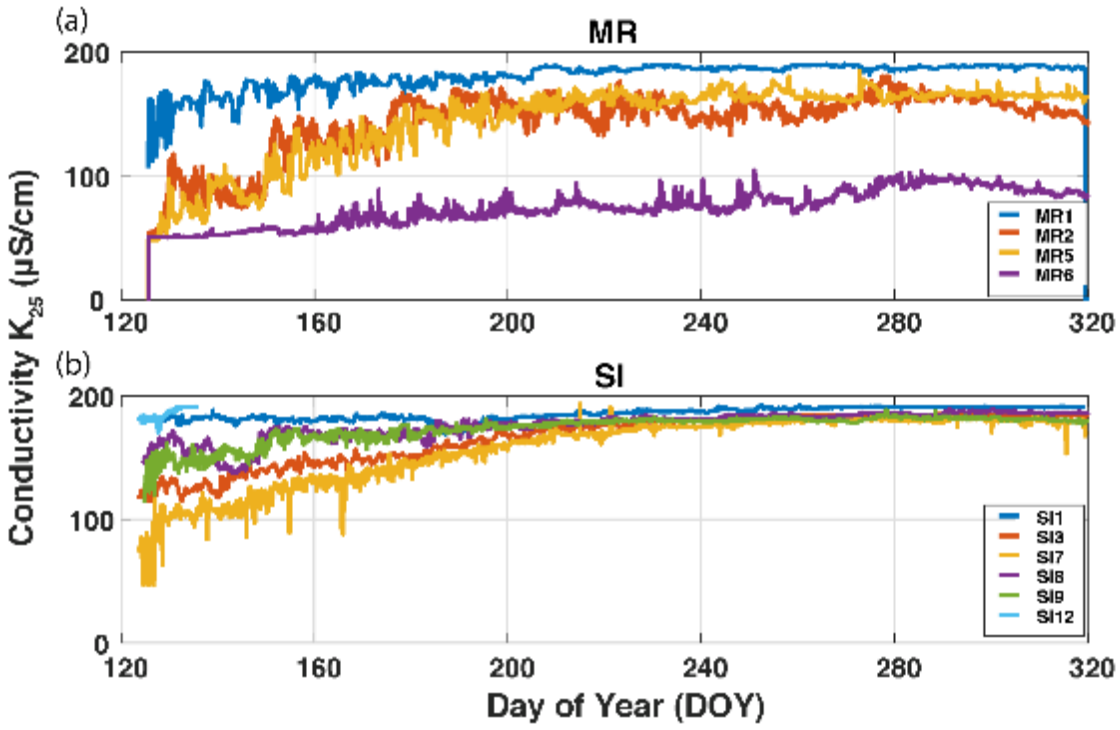

410

411 **Figure 6.** Time series of specific conductivity measured at moorings in both (a) MR and (b) SI.
412 During late spring and summer in 2015, specific conductivity distributions show the existence of
413 a spatial conductivity gradient in both regions. The gradient is wider at MR compared to SI, and
414 there is more seasonality in conductivity at the SI site.

415 Variable specific conductivity levels in nearshore zones are driven by advection and
416 mixing of freshwaters from land with the bay waters. Thus, we examined the temporal variability
417 of river influx to Georgian Bay (Figure S1). River discharge rates used in our analysis are estimates
418 from the gauges upstream from the lake. In 2015, river discharge in both study sites show a

seasonal variability. For both study sites, the maximum daily average river discharge peaked during spring and gradually lowers over the summer. The maximum daily average discharge for MR is 177 m^3/s (DOY 117) and for SI, it is 45 m^3/s (DOY 112). The daily average river discharge during summer (DOY ~162-287) was much lower at 2.8 m^3/s and 1.77 m^3/s for MR and SI, respectively. The annual average of daily river discharge for MR is comparatively high with a value of 15.92 m^3/s whereas SI has a lower annual average discharge of 4.39 m^3/s. Hence, on average high river volume flux at MR limits the influx of lake water in shallow water embayment and results in a broader conductivity gradient.

3.2 Physical Conditions Shaping the Solute Gradients in Eastern Georgian Bay

The stratification in the coastal zone of EGB is a function of time and largely depends upon the local depth relative to the main thermocline of Georgian Bay. In 2015, thermal stratification at the outer extent of the coastal zones of both regions began in early to mid-June (DOY 160-170; MR1 and SI4) (Figure 7a-d) with a coherent seasonal thermocline varying from 5 to 20 m. The mean depth of the thermocline was in the range of 10-12 m and the maximum temperature reached 20 ^{0}C by mid-August and ranged from 6 ^{0}C to 20 ^{0}C (see Figure 2c-d for locations). The periodic intrusion of offshore hypolimnetic water and short-term variability in the thermocline correlated with wind suggested weak upwelling events. There was more limited or no thermal stratification within shallow embayed areas at sites MR7 and SI3 (Figure 7a, c), where depths were shallower than thermocline in the main basin.

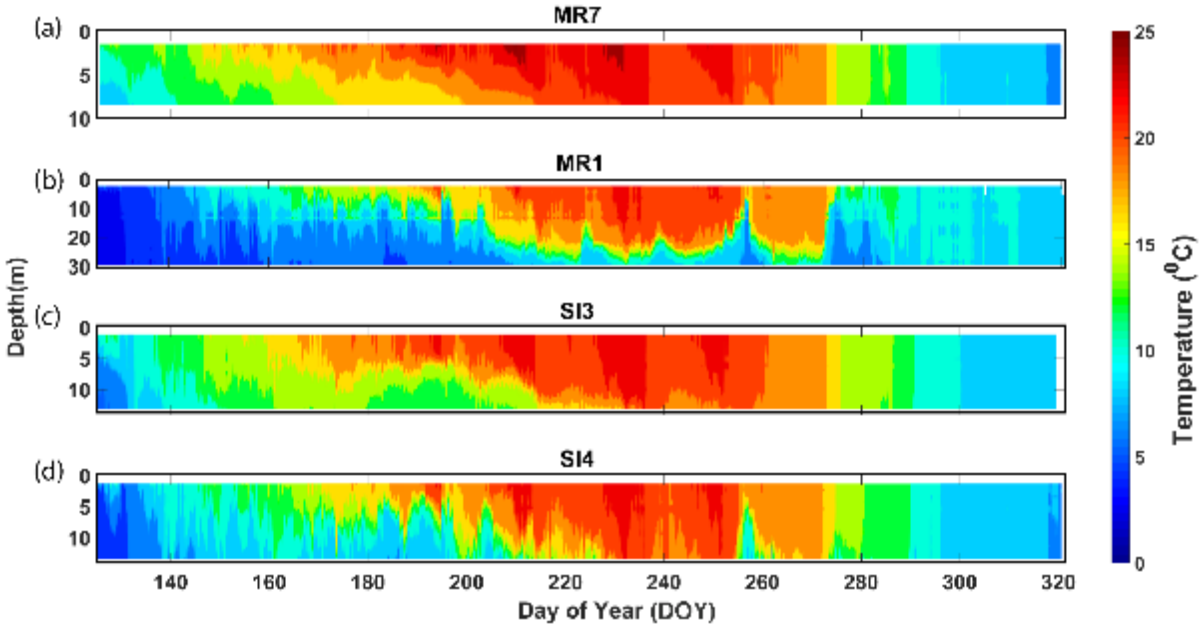

Figure 7. Observed temperature time series derived from thermistor chains at (a) MR7, (b) MR1, (c) SI3, and (d) SI4. The MR7 is located inside the embayment near the river mouth of the Moon River region. Similarly, the SI3 is located inside the elongated channel near the Shawanaga River mouth. The MR1 and SI4 are located in the open waters of EGB.

The currents derived from upward-looking bottom-mounted ADCP sensors show an oscillatory pattern in both SI and MR (Figure S2a-e). These alternating currents, on average, vary up to 0.2 ms^{-1} and have variable time scales. Currents with large speed variability were seen in the open bay (e.g., MR1, SI1, and SI8) compared to those observed in shallow embayments (e.g., MR3 and SI6). To determine the mode of transport (barotropic or baroclinic flow) of the oscillatory motion, we applied EOF analysis to horizontal currents. During the stratified season (DOY 162-287), at a sensor located in the open bay at Shawanaga Inlet (SI1), the first two modes of north-south velocity show ~87% of the total variance (Figure 8a-b and Figure S3) with mode 1 accounting for ~70% of this variability. There was no change in the sign of the amplitude of the EOF mode 1 (Figure 8a) with increasing depth and decreasing magnitude. This suggests that the whole water column flows in one direction with no vertical gradient equivalent to a barotropic flow. The second mode (Figure 9b) shows changes in the sign from positive to negative at about 9 m from the surface indicating a division of the water column into two distinctive portions (surface and sub-surface) where surface flow is opposite to the sub-surface flow. The first principal component time series (Figure S3b) shows a sign change from negative to positive in amplitude resembling the oscillatory motion seen in Figure S2 which depicts reversal of the direction of water column flow. Only the EOFs for north-south currents at SI are shown here (Figure 8a-f). The north-south currents in SI approximate the landward and open bay-ward movement of water at the mouth of the southern channel of Shawanaga Island through which much of the mixing across the coastal zone occurs as reflected in ADCP measurements at SI8 and SI6. Similar characteristics were seen in the EOF analysis for east-west velocity. East-west currents approximate the landward and open bay-ward movement of water at SI1 and other areas of SI depending on the topographic orientation of channels and islands.

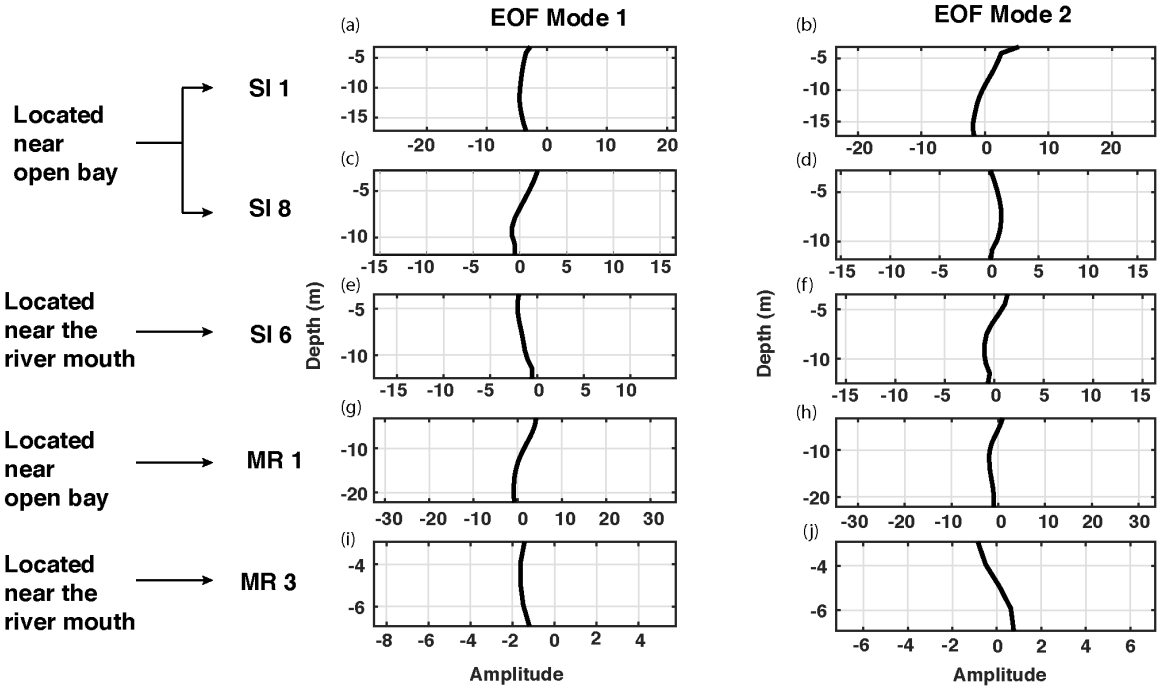

Figure 8. The first and second modes of EOF analysis to SI 1, SI 8, SI 6, MR 1, and MR 3. For the SI region, EOF analysis is performed for north-south currents. The individual EOF modes and

principal component time series for SI can be found in Figures S3-S5. For the MR region, EOF analysis was performed for east-west currents. Individual EOF modes and principal components for MR are shown in Figures S6-S7.

Although SI1 represents the motion in the open bay, there are reefs between SI1 and the southern inlet of Shawanaga Island that may affect how well the ADCP measurements represent the exchange into the complex of embayments of the SI areas. Data collected at the sensor located near the southern entrance to Shawanaga Inlet adjacent to the open bay (SI 8) may better describe water exchange with Shawanaga Inlet. At SI8, the first two modes of the north-south currents of the EOF accounted for ~70% of total variability with the first contributing 40% of the variance (Figure 8c-d and Figure S4). The first mode shows a sign change from positive to negative at mid-depth (~7m) indicating bidirectional flow with the surface and sub-surface water moving in opposing directions suggesting a baroclinic flow. The second mode amplitude is positive in the vertical indicating the whole water column moving in one direction as a barotropic flow.

At a sensor located deep within Shawanaga Inlet near a river mouth (SI 6), the first two modes of the EOF analysis mode 1 and 2 accounted for ~64% and ~19% of the variability, respectively (Figure 8e-f and Figure S5). The amplitude is negative through the water column in the first mode indicating that the entire water column flows in either north or south direction. Mode 2 of EOF shows a sign change from positive to negative in the vertical indicating bidirectional flow at about 6 m from the surface.

For MR, we performed EOF analysis for east-west currents (Figure 8g-j) because east-west currents best approximate landward and open bay-ward motion of water in this region. The first two modes of the EOF for MR1 in the open bay is accounted for ~77% of the total variance with ~54% attributed to mode 1 (Figure 8g-h and Figure S6). There was a reversal in sign of the amplitude from positive to negative at mid-depth (~13 m from the surface) in mode 1 indicating opposed flows over the water column. The EOF pattern of mode 2 was similar to mode 1. The first two modes of the EOF for MR 3 located inside a shallow embayment near a river mouth depicted patterns similar to SI6 also located within an embayment and near a river mouth (Figure 8i-j and Figure S7). Mode 1 accounted for ~77% of the total explained variance of ~91%. The first mode is negative over depth compared to a sign change at mid-depth in the second mode.

The EOF analysis suggests that barotropic exchanges are more typical in locations within embayments, possibly throughout the coastal zone when considered in light of the times of the year when the water column is unstratified, however, baroclinic flows were frequent in the open lake and the interface areas between embayments and the open lake.

The barotropic and baroclinic transport processes in EGB exhibited hourly to seasonal variability in occurrence and intensity. The energy spectrums of the depth average velocities of all stations (Figures S8 and S9) show a flat peak around 4 days (~ 0.009 cph) and a spectral minimum at around ~ 30 h (~ 0.03 cph). The spectral minimum is interpreted as the transfer of energy from large-scale circulations to small-scale fluctuations (Rao and Murthy, 2001). Therefore, for our analysis, we high pass filtered the time series of velocities (east-west, north-south) to capture motions with periods less than 24 h which include high-frequency oscillations such as inertial fluctuations that contributes to dispersion of solutes (Murthy and Dunbar, 1981; Rao and Murthy, 2001).

Individual analysis of FFT for both high-pass filtered east-west (Figure 9a, c) and north-south (Figure 9b, d) current velocities at SI and MR shows significant peaks at around 24.381 h (0.04 cph), 17.07 h (~0.059 cph), 14.2 h (0.07 cph), 12. 488 h (~0.08 cph), and 2.4 h (~0.42 cph). All the above peaks are previously observed in Georgian Bay (Schwab and Rao, 1977). The 24.381 h and 12.488 h peaks are for diurnal and semidiurnal variability. The ~17 h peak is due to inertial oscillations. The 14.2 h peak corresponds to the Georgian Bay mode 1 (free mode oscillation) observed in Schwab and Rao (1977). Hence, the advection (transport) of solutes is mainly forced by the surface elevation gradient caused by diurnal winds and inertial oscillations.

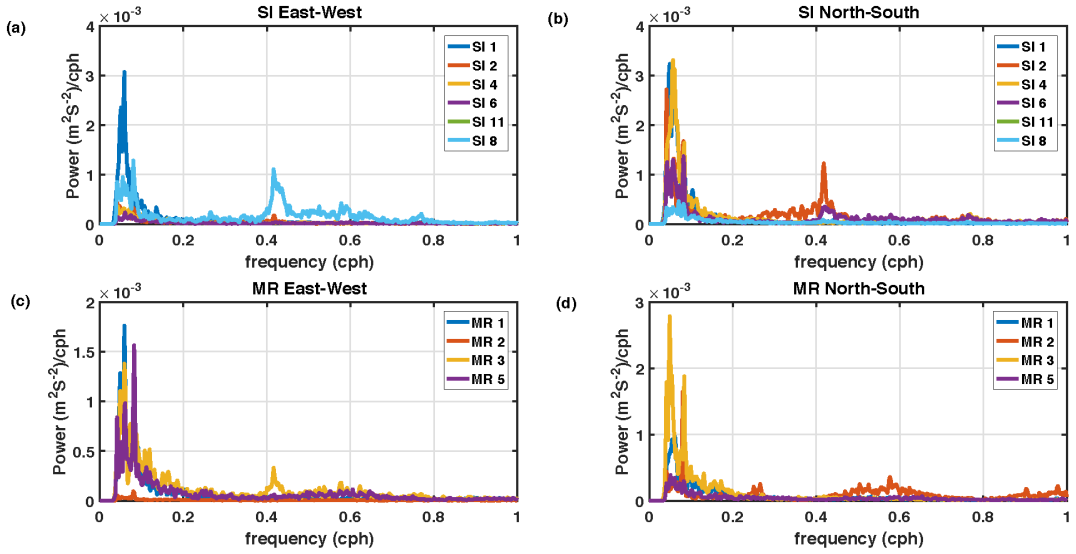

Figure 9. The power spectrum for high-pass filtered depth-averaged east-west and north-south current velocities observed for SI and MR. The individual FFT peaks for each station are given in Figures S11-S12.

During each diurnal cycle, the excursion path oscillates onshore-offshore (Figure S10a-b) which resembles the oscillatory motion observed in velocity time series (Figure S2). Daily excursion length at SI showed (red contour in Figure S10c) an average of 80 m with a maximum and standard deviation of 400 m and 60 m, respectively. For MR (blue contour in Figure S10c), the daily average, maximum, and standard deviation were 100 m, 290 m, and 66 m, respectively. On average, MR has a large excursion length than that at SI.

4 Discussion

The coastal areas of large lakes, often referred to as the nearshore, support a unique component of lake ecosystems where tributary loading affects the nutrient and solute concentrations and influences natural habitat selection by aquatic species. The distinctive physical processes at the coastline in combination with variable tributary discharge lead to more variable distributions of nutrients and solutes compared to offshore waters. Studies in marine archipelagos resembling in part the EGB archipelago such as the Baltic Sea have shown that the flow is estuarine in nature and is driven by a combination of river forcing, longitudinal density gradients, winds, and weak tides (Suominen et al., 2010). The flow regime of the open waters of EGB adjacent to

538 the coastline is mainly wind-driven (Schwab and Rao, 1977; Bennett, 1988) and with weak tides,
539 generally with a maximum range of less than 5 cm over 24 h period. The added combinations of
540 river forcing and internal mixing within the coastal zone can create longitudinal density gradients.
541 It may be useful to think of many inlets in EGB as being freshwater estuaries where, water quality
542 is driven by a combination of loading, horizontal, and vertical mixing.

543 In this study, we examined the horizontal mixing processes responsible for nearshore
544 gradients of solutes that limit the spatial distribution of aquatic organisms as demonstrated here by
545 the invasive dreissenid mussels. Our field observations demonstrate a more limited distribution of
546 dreissenid mussels at sites located within embayed areas compared to those close to the open bay.
547 Mussel abundance was strongly related to water column specific conductivity at the time of the
548 benthic surveys ranging from July to September such that mussels were generally not found at
549 specific conductivities less than 140 μS/cm. In EGB, conductivity is strongly determined by
550 concentrations of dissolved calcium and can be used to predict calcium concentrations with a
551 conductivity of 140 μS/cm equating to about 14.8 mg/L of calcium. In another field study in SW
552 Lake Superior where calcium levels ranged from 11 to 14 mg/L, Trebitz et al. (2019) reported little
553 detection of dreissenid mussels. Adult mussels or their DNA were not detected after extensive
554 sampling, however low densities of veliger were detected which the authors suggested were
555 transported from a river estuary with mussels.

556 4.1. Sensitivity of mussels to calcium concentrations.

557 The literature suggests that survival, growth, and reproductivity are sensitive to varying
558 ranges of calcium concentration. Baldwin et al. (2012) using lab bioassays with field-collected
559 mussels and low calcium lake water asserted that growth and reproductive success were reduced
560 at concentrations of Ca below what adult mussels could survive. Survival of juvenile mussels was
561 affected below 12 mg/L compared with 6 mg/L for adults. Their experiments suggested that
562 exposure to low calcium water will be most inhibitive to the establishment of mussel populations
563 during the reproductive period from when zygotes are spawned to when veligers, the planktonic
564 early life stage of dreissenid mussels, are present. Failure to produce young of year juvenile
565 mussels due to exposure to non-tolerable calcium levels 12 to 13 mg/L during the veliger stage
566 reported by Baldwin et al. (2012) appears to be a possibility in eastern Georgian Bay. An additional
567 factor that possibly affected the establishment of populations is sub-lethal effects on growth rate
568 and reproductive success which Baldwin et al. (2012) reported decreased with increasing calcium
569 levels up to 18 to 24 mg/L. Similarly, Davis et al. (2015) observed reduced mussel growth at low
570 non-inhibitive Ca concentrations and speculated that over a seasonal period, mussels might not
571 survive because of poor growth that compromised the population's ability to reproduce and persist.

572 The correspondence between mussel occurrence and conductivity reported here is likely
573 attributable to physiological effects of low alkalinity water, possibly related to calcium levels,
574 however, the timing of the key interactions between solute gradients over the study area and
575 potential physiological effects is uncertain. The conductivity data depicting mussel occurrence
576 were collected from July to September, a period when conductivity was at seasonal highs (Figure
577 6) and when the presence of the more sensitive veligers stage is anticipated. Pothoven and Elgin
578 (2019) studied seasonal distribution patterns of veligers in Lake Michigan reporting peak veliger
579 abundance in nearshore areas from June to November. The lower conductivity and calcium levels
580 experienced in the more embayed areas during the high river-discharge periods of spring, early

summer, and fall when coastal solute gradients are wider occur at times when veligers are possibly less abundant. Effects of low alkalinity water at these times may be more on adult survival and growth may more affect mussel distribution and abundance. When considered from the perspective of a fixed location over time the adverse effects of low calcium on mussel occurrence may result at multiple points in time and at multiple points in the mussel life cycle. Our empirical relationship between mussel occurrence and conductivity captures an integration of these possibilities and depicts the outcome in terms of the upper range of conductivity - calcium that sites likely experience over the seasonal dynamics of the coastal solute gradient.

4.2. Effect of substrate type on mussel distribution.

A co-varying factor with conductivity also related to dreissenid mussel distribution was substrate type. Overall, mussels were less abundant on soft compared with hard substrate and mussel abundance on soft substrate was unrelated to conductivity above a threshold above which they were found, a threshold similar to hard substrate. The diminished exposure within embayments contrasting with the high exposure of the open lake sites results in the hard and soft substrates being disproportionally distributed more over the high and low ends of the EGB coastal solute gradients, respectively. Also, mussel colonization on soft substrate at inshore depths typically requires mussel attachment sites on erratic hard particles within the sediment matrix which serve as a seeding site for rafting of aggregates of mussels. Arguably the low mussel abundance as seen over the lower range of the solute gradient would make colonization of soft sediment more difficult in a relative sense to hard substrate.

4.3. Effect of horizontal mixing on setting nutrient gradients across the coastal zone.

The seasonal dynamics of the solute gradient extending across the coastal zone were identified from the data collected in spatial and temporal water quality surveys. A similar conductivity gradient across the coastal zone was reported by Bocaniov et al. (2013) in Twelve Mile Bay in EGB. Gradients of solutes (conductivity) in EGB are a result of transport and mixing of solutes and must be viewed in the context of advection (transport) and dispersive (mixing) processes which shape the gradients over the coastline. The EOF analysis showed the flow in shallow embayments is predominantly barotropic and is baroclinic near the open bay end of the archipelago. The power spectrum analysis demonstrated that the system is mainly forced by diurnal winds and inertial oscillations. This effect of the circulation is analogous to an estuarine flow. While baroclinic flow in the open bay results from the density gradient due to thermal stratification, the barotropic flow in the shallow embayments results from the surface elevation gradient by the wind setup and river inflow. In this estuarine style flow, the mixing of low conductivity river waters occurs with high conductivity open Georgian Bay waters. The degree of mixing of solutes from high conductivity waters largely depends on the river inflow. If the river discharge is high, the barotropic flow can flush the freshwater out from the shallow embayments such that, mixing of freshwater occurs farther away from the river mouth. The opposite occurs when river discharge is slow to moderate such that barotropic flow brings high conductivity waters from the open bay and mixes quickly with the freshwater.

4.4. Estimation of horizontal dispersion in EGB.

Horizontal mixing is a result of turbulence (fluctuations) in the velocity field and shear in

the advective flow field (Rao et al., 2008). It can be explained by a mixing zone where it is a function of the horizontal dispersion coefficient parameter. The variability of predicted horizontal dispersion coefficient in east-west and north-south directions for both MR and SI show that the horizontal dispersion coefficients get larger when moving from the shallow embayments (MR3 and SI6) towards the open bay (MR1, SI8, SI1) (**Table 1).** The estimated horizontal dispersion coefficient varies with depth for sensors located in the open bay contrasting with the approximately uniform K_x in shallow embayments (Figure 10).

Table 1. The predicted depth independent horizontal dispersion coefficient (K_x) from current measurements.

	East-West (units $\mathbf{m^2s^{-1}}$)	North-South (units $\mathbf{m^2s^{-1}}$)
MR 1	1.91	1.71
MR 3	0.85	1.08
SI 1	3.86	4.49
SI 8	1.38	1.02
SI 6	0.43	1.23

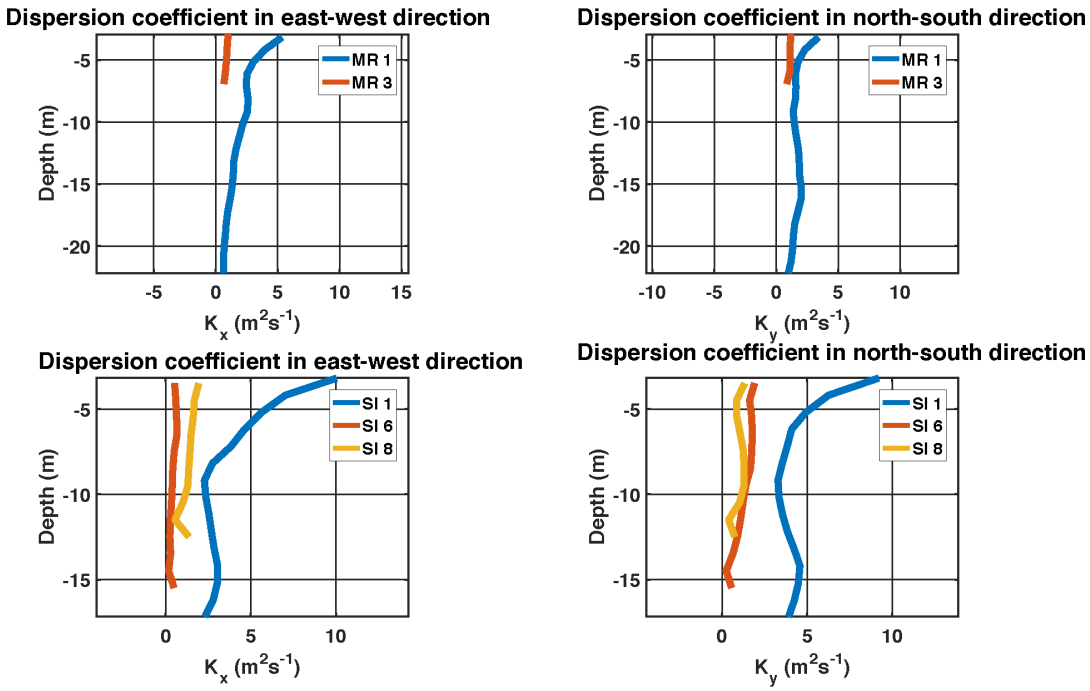

Figure 10. Vertical variability of computed horizontal dispersion coefficient. (a) in the east-west

direction of MR. (b) in the north-south direction of MR. (c) in the east-west direction of SI. (b) in the north-south direction of SI.

4.5. Estimation of up-estuary intrusion length scale as a measure of setting the coastal mixing zone.

In an estuarine flow, the gradient of solutes results from two interactive processes: the advection due to exchange between low conductivity river waters with high conductivity open bay waters, and, mixing of solutes within. During advection, the distance over which up-estuary intrusion of relatively "salty" water, without mixing with the river, can be described as an up-estuary intrusion length scale (analogous to the theoretical intrusion length scale in Zimmerman and Kjerfve, 1988). In contrast, a mixing zone for this freshwater estuary can be introduced as the length scale over which the mixing of two waters occurs. In other words, the mixing zone is derived by subtracting the up-estuary intrusion length scale from the total length scale of the freshwater estuary (as shown in Figure 1). The intrusion length scale at the quasi-steady-state (averaged over a dominant cycle ~ 24 h) can be defined as the ratio of horizontal dispersion ($\boldsymbol{K_x}$)to the velocity generated by the mean volume transport ($\boldsymbol{Q/A}$) where, $\boldsymbol{Q}$ is the mean volume transport at the up-estuary end and it is the sum of river discharge ($\boldsymbol{Q_R}, \mathbf{m^3 s^{-1}}$) and net transport from general land runoff ($\boldsymbol{Q_T}, \mathbf{m^3 s^{-1}}$), $\boldsymbol{A}$ is the cross-sectional area ($\mathbf{m^2}$) of the channel (MacCready, 2004; MacCready, 2007; Gay and O'Donnell, 2007). It is important to note that at the quasi-steady-state (during each 24 h cycle), the average of the high-frequency fluctuations becomes null and hence, an average velocity field is generated by the net volume transport. In general, for SI and MR, the net volume transport from land runoff is small compared to the river discharge from the major rivers ($\boldsymbol{Q_T \ll Q_R,\ Q = Q_R}$). Based on daily average river inflow (from DOY 160-280, Figure 11a), the up-estuary intrusion length scale ($\boldsymbol{AK_x/Q_R}$) for SI varies between 3 – 37 km (Figure 11b) where we assumed the mean width of the SI channel (W) as 3 km, mean depth (H) as 5.8 m, and the depth independent horizontal dispersion coefficient ($\boldsymbol{K_x}$) in the north-south direction at SI 8 as 1.02 m^2s^{-1}. For MR, we assumed the mean channel width (W) as 2.2 km, mean depth as 7.6 m, and the depth independent $\boldsymbol{K_x}$ in the east-west direction at MR 1 as 1.91 m^2s^{-1}. Thus, the up-estuary intrusion length scale in MR varies between 2 – 15 km (Figure 11b).

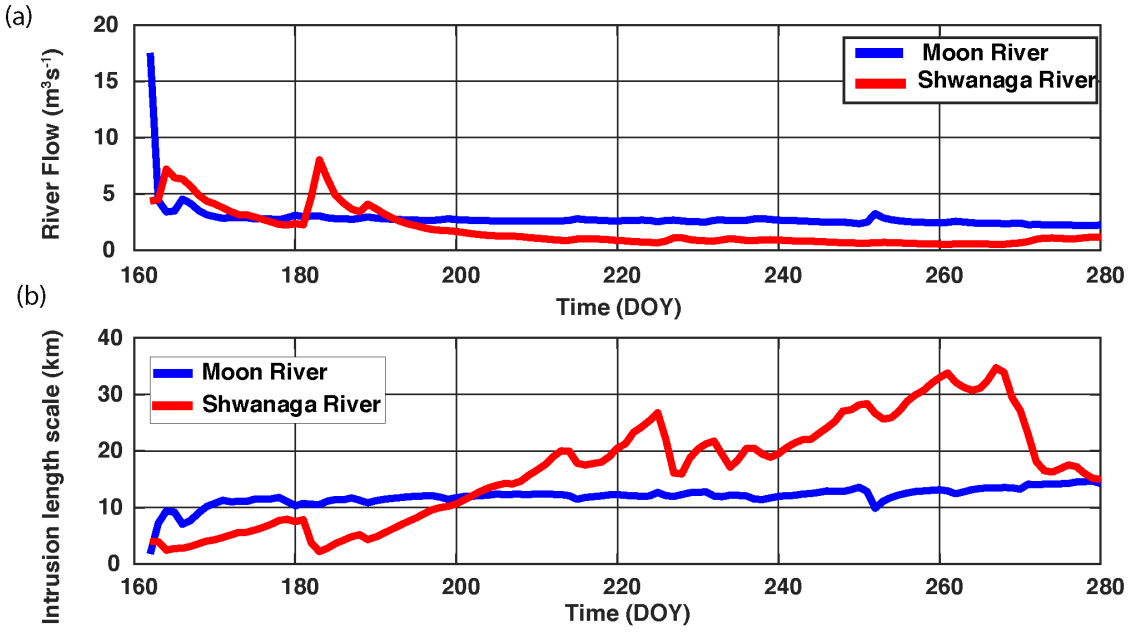

Figure 11. (a) Variability in river discharge in SI and MR. (b) Up-estuary intrusion length scale computed from the parametrization ($\boldsymbol{AK_x/Q_R}$).

4.5. Effect of seasonal and regional variability of up-estuary intrusion length scale.

For each region (either SI or MR), the seasonal variability in the up-estuary intrusion length scale is proportional to $\boldsymbol{1/Q_R}$. When the river inflow is high, such inverse proportionality leads to slow mixing of low conductivity waters from the rivers with the ambient. This implies a long mixing zone where low conductivity waters advect (transport) further towards the open bay. The opposite occurs when the river inflow is low, meaning, low conductivity river waters mix quickly with the ambient while creating a short mixing zone. On the other hand, a regional comparison between SI and MR reveals that SI has high variability in estimated daily river inflow compared to MR. Hence, the up-estuary intrusion length scale in SI shows significant temporal fluctuations compared to that of in MR. River inflow in MR (Figure 11a) from mid-July (DOY 200) to early October (DOY 280) is approximately three times bigger than the estimated inflow to SI. It is also evident that the up-estuary intrusion length scale for the same period in SI is relatively high compared to MR (Figure 11b). Therefore, on average MR has a low intrusion length scale (~12 km) compared to the average up-estuary intrusion length scale for SI (~17 km). This suggests that the mixing zone in MR is long and almost constant throughout the stratified season. In comparison, the mixing zone in SI shortens towards the end of the stratified season. This is also evident in the time series of the conductivity measured at moorings (Figure 6). This parameterization is also true for areas where there are no major rivers but sufficient land runoff generally in the spring ($\boldsymbol{Q_R \sim 0,\ Q = Q_T}$). In such a scenario, the up-estuary intrusion length scale is proportional to $\boldsymbol{1/Q_T}$. Hence, the higher the land runoff the lower the intrusion length scale and the long mixing zone. The opposite occurs when the land runoff is small.

From our analysis, it is clear that the advection-mixing processes are key to understanding

685 the length scale of the mixing zone and lake intrusion zone which set the coastal solute gradients.
686 Within that solute gradient there lies a threshold solute concentration suitable for successful growth
687 of dreissenid mussels. Variability of conductivity levels within the mixing zone will determine the
688 locations for threshold conditions where an imaginary boundary for landward invasion of
689 dreissenid mussels exists. The intrusion of open bay waters (conductivity is usually at 180-190
690 μS/cm) into the shallow embayments can be expected from a long up-estuary intrusion length scale
691 thus, mixing of solutes can generate a solute concentration above the threshold values (e.g., SI in
692 Figure 3a). The opposite occurs when there is a short up-estuary intrusion length scale. Such that,
693 mixing of freshwater with relatively "salty" water is dampened. Therefore, reaching the threshold
694 levels of calcium required for successful growth of dreissenid mussels is difficult. Therefore,
695 landward invasion of dreissenid mussels is limited (e.g., MR in Figure 3d).

696 **5 Conclusion**

697 The observed gradients of conductivity in the nearshore zones of EGB of Lake Huron
698 suggest that low calcium concentrations adversely affect dreissenid mussels distribution and
699 abundance. The gradients of solutes in the mixing zone of river mouths of this fragmented
700 archipelago are similar to an estuary, where the diurnal winds and inertial motions driven
701 circulation controls the dispersion of low conductivity river waters flowing from the Canadian
702 Shield. A short mixing zone results in a weak down-estuary solute gradient. Therefore, the
703 intrusion of open bay waters suggests a favourable condition for successful up-estuary invasion of
704 dressenid mussels. The opposite occurs when the down-estuary solute gradient is strong resulting
705 from a long mixing zone such that, there are small upstream intrusions of invasive mussels.

706 This study provides a foundation for estimation of mixing zones (in terms of up-estuary
707 intrusion length scale) between the river and open lake that is relevant to other water quality and
708 ecosystem concerns in other freshwater estuaries. A similar analysis can be used to estimate the
709 residual accumulation or residual outflow of parameters such as organic and inorganic substances
710 from the rivers, such as road salts or phosphorous loadings. If the intrusion length scale is small,
711 then there would be a long mixing zone from the up-estuary end. Our analysis provides insight on
712 mixing conditions over the coastal margin between the mouths of the river and adjacent lake which
713 influence biological distributions over the fragmented coastline.

714 **Acknowledgments**

715 The contributions of Brian Thorburn, Ryan Mototsune, Wendy Page of the Great Lakes field unit
716 of the Ontario Ministry of the Environment, Conservation and Parks in the undertaking of field
717 work supporting this study is gratefully acknowledged. The field data collections were conducted
718 by MECP as part of the Province's Great Lake monitoring program. We thank Tim Moran, Jeff
719 Houtby and Terry Dolbear of Pollutec limited who conducted the diver-based sampling of
720 dreissenid mussels under contract to MECP.

721 Funding to Mathew Wells from Canada-Ontario Agreement program of MECP in part supported
722 this study.

723

Data Availability Statement

Previously unpublished data are available at http://doi.org/10.5281/zenodo.4744857.

References

Baldwin, B. S., Carpenter, M., Rury, K., & Woodward, E. (2012). Low dissolved ions may limit secondary invasion of inland waters by exotic round gobies and dreissenid mussels in North America. *Biological Invasions*, *14*(6), 1157-1175.

Barton, D. R., Howell, E. T., & Fietsch, C. L. (2013). Ecosystem changes and nuisance benthic algae on the southeast shores of Lake Huron. Journal of Great Lakes Research, 39(4), 602-611.

Bennett, E. B. (1988). On the physical limnology of Georgian Bay. In *Limnology and Fisheries of Georgian Bay and the North Channel Ecosystems* (pp. 21-34). Springer, Dordrecht.

Berst, A. H., and Spangler, G. R. (1973). *Lake Huron: the ecology of the fish community and man's effects on it*. Great Lakes Fishery Commission.

Bocaniov, S. A., Barton, D. R., Schiff, S. L., & Smith, R. E. (2013). Impact of tributary DOM and nutrient inputs on the nearshore ecology of a large, oligotrophic lake (Georgian Bay, Lake Huron, Canada). *Aquatic Sciences*, *75*(2), 321-332.

Botts, P. S., Patterson, B. A., & Schloesser, D. W. (1996). Zebra mussel effects on benthic invertebrates: physical or biotic? *Journal of the North American Benthological Society*, *15*(2), 179-184.

Budd, J. W., Drummer, T. D., Nalepa, T. F., & Fahnenstiel, G. L. (2001). Remote sensing of biotic effects: Zebra mussels (Dreissenid mussels polymorpha) influence on water clarity in Saginaw Bay, Lake Huron. *Limnology and Oceanography*, 46(2), 213-223.

Campbell, S. D., & Chow-Fraser, P. (2018). Models to predict total phosphorus concentrations in coastal embayments of eastern Georgian Bay, Lake Huron. *Canadian Journal of Fisheries and Aquatic Sciences*, *75*(11), 1798-1810.

Casagrande, G., Stephan, Y., Varnas, A. C. W., & Folegot, T. (2011). A novel empirical orthogonal function (EOF)-based methodology to study the internal wave effects on acoustic propagation. *IEEE Journal of Oceanic Engineering*, *36*(4), 745-759.

Csanady, G. T. (1968). Wind-driven summer circulation in the Great Lakes. *Journal of Geophysical Research*, *73*(8), 2579-2589.

Csanady, G. T. (1963). Turbulent diffusion in Lake Huron. *Journal of Fluid Mechanics,* 17(3), 360-384.

Davis, C. J., Ruhmann, E. K., Acharya, K., Chandra, S., & Jerde, C. L. (2015). Successful survival, growth, and reproductive potential of quagga mussels in low calcium lake water: is there uncertainty of establishment risk? *Peer J*, 3, e1276.

Gay, P. S., & O'Donnell, J. (2007). A simple advection-dispersion model for the salt distribution in linearly tapered estuaries. *Journal of Geophysical Research: Oceans*, 112(C7). doi:10.1029/2006JC003840.

Grigorovich, I. A., Korniushin, A. V., Gray, D. K., Duggan, I. C., Colautti, R. I., & MacIsaac, H. J. (2003). Lake Superior: an invasion coldspot?. *Hydrobiologia*, *499*(1-3), 191-210.

Harrington, M. W. (1895). Surface currents of the Great Lakes: as deduced from the movements of bottle papers during the seasons of 1892, 1893, and 1894. *United States Dept. of Agriculture. Weather Bureau. Bulletin* 12 pp.

777 Hay, J. S., & Pasquill, F. (1959). Diffusion from a continuous source in relation to the spectrum
778 and scale of turbulence. In *Advances in geophysics* (Vol. 6, pp. 345-365). Elsevier.

779 Hecky, R. E., Smith, R. E., Barton, D. R., Guildford, S. J., Taylor, W. D., Charlton, M. N., &
780 Howell, T. (2004). The nearshore phosphorus shunt: a consequence of ecosystem engineering by
781 dreissenids in the Laurentian Great Lakes. *Canadian Journal of Fisheries and Aquatic*
782 *Sciences*, *61*(7), 1285-1293.

783 Higgins, S. N., Malkin, S. Y., Howell, T. E., Guildford, S. J., Campbell, L., Hiriart-Baer, V., &
784 Hecky, R. E. (2008). An ecological review of Cladophora glomerata (CHLOROPHYTA) in the
785 Laurentian Great Lakes 1. *Journal of Phycology*, *44*(4), 839-854.

786 Higgins, S. N., & Zanden, M. V. (2010). What a difference a species makes: a meta–analysis of
787 dreissenid mussel impacts on freshwater ecosystems. *Ecological monographs*, *80*(2), 179-196.

788 Higgins, S. N., Pennuto, C. M., Howell, E. T., Lewis, T. W., & Makarewicz, J. C. (2012). Urban
789 influences on Cladophora blooms in Lake Ontario. *Journal of Great Lakes Research*, *38*, 116-123.

790 Howell, E. T., Marvin, C. H., Bilyea, R. W., Kauss, P. B., & Somers, K. (1996). Changes in
791 environmental conditions during Dreissenid mussels colonization of a monitoring station in eastern
792 Lake Eric. *Journal of Great Lakes Research*, *22*, 744-756.

793 Howell, E. T. (2004). Occurrence of nuisance benthic algae on the southwestern shores of Lake
794 Huron, 2003. In *Technical Memo*. Ontario Ministry of the Environment.

795 Howell, E. T., Barton, D. R., Fietsch, C. L., & Kaltenecker, G. (2014). Fine-scale nutrient
796 enrichment and water quality on the rural shores of Southeast Lake Huron. *Journal of Great Lakes*
797 *Research*, *40*(1), 126-140.

798 Johengen, T. H., Nalepa, T. F., Fahnenstiel, G.L., & Goudy, G. (1995). Nutrient changes in
799 Saginaw Bay, Lake Huron, after the establishment of the zebra mussel (Dreissenid mussels
800 polymorpha). *Journal of Great Lakes Research*, *21*, 449-464.

801 Jones, L.A. & Ricciardi, A. (2005) Influence of physicochemical factors on the distribution and
802 biomass of invasive mussels in the St. Lawrence River. *Canadian Journal of Fisheries and Aquatic*
803 *Sciences*, *62*, 1953–1962.

804 Kaihatu, J. M., Handler, R. A., Marmorino, G. O., & Shay, L. K. (1998). Empirical orthogonal
805 function analysis of ocean surface currents using complex and real-vector methods. *Journal of*
806 *Atmospheric and oceanic technology*, *15*(4), 927-941.

807 Kawamura, R. (1994). A rotated EOF analysis of global sea surface temperature variability with
808 interannual and interdecadal scales. *Journal of Physical Oceanography*, *24*(3), 707-715.

809 Levitus, S., Antonov, J. I., Boyer, T. P., Garcia, H. E., & Locarnini, R. A. (2005). EOF analysis of
810 upper ocean heat content, 1956–2003. *Geophysical Research Letters*, *32*(18).

811 MacCready, P. (2004). Toward a unified theory of tidally-averaged estuarine salinity structure.
812 *Estuaries,* 27(4), 561-570.

813 MacCready, P. (2007). Estuarine adjustment. *Journal of Physical Oceanography*, *37*(8), 2133
814 2145.

815 Mackie, G. L (2004), Applied Aquatic Ecosystem Concepts, 2nd ed. Dubuque: Kendall/Hunt
816 Publishing Company, 784 pp.

817 McMahon, R. F. (1996). The physiological ecology of the zebra mussel, Dreissenid mussels
818 polymorpha, in North America and Europe. *American Zoologist*, *36*(3), 339-363.

819 Morrison, J. E., and Smith, J. A. (2001). Scaling properties of flood peaks. *Extremes*, *4*(1), 5-22.

820 Murthy, C. R. (1976). Horizontal diffusion characteristics in Lake Ontario. *Journal of physical*
821 *oceanography*, *6*(1), 76-84.

822 Murthy, C. R., & Dunbar, D. S. (1981). Structure of the flow within the coastal boundary layer of
823 the Great Lakes. *Journal of Physical Oceanography*, *11*(11), 1567-1577.

824 Nalepa, T. F., & Fahnenstiel, G. L. (1995). Dreissenid mussels polymorpha in the Saginaw Bay,
825 Lake Huron ecosystem: overview and perspective. *Journal of Great Lakes Research* 21(4), 411-
826 416.

827 Nalepa, T. F., Fanslow, D. L., Pothoven, S. A., Foley III, A. J., & Lang, G. A. (2007). Long-term
828 trends in benthic macroinvertebrate populations in Lake Huron over the past four
829 decades. *Journal of Great Lakes Research*, *33*(2), 421-436.

830 Nalepa, T. F. (2010). An overview of the spread, distribution, and ecological impacts of the quagga
831 mussel, Dreissenid mussels rostriformis bugensis, with possible implications to the Colorado River
832 system. Proceedings, Colorado River Basin Science and Resource Management Symposium.
833 Coming Together, Coordination of Science and Restoration Activities for the Colorado River
834 Ecosystem, Scottsdale, AZ, November 18–20, 2008. *U.S. Geological Survey Scientific*
835 *Investigations Report:* 2010–5135.

836 Nalepa, T. F., Riseng, C. M., Elgin, A. K., & Lang, G. A. (2018). Abundance and Distribution of
837 Benthic Macroinvertebrates in the Lake Huron System: Saginaw Bay, 2006-2009, and Lake
838 Huron, Including Georgian Bay and North Channel, 2007 and 2012. *NOAA Technical*
839 *Memorandum GLERL* ; 172

840 Pothoven, S. A., & Elgin, A. K. (2019). Dreissenid veliger dynamics along a nearshore to offshore
841 transect in Lake Michigan. *Journal of Great Lakes Research*, *45*(2), 300-306.

842 Pothoven, S. A., Nalepa, T. F., Schneeberger, P. J., & Brandt, S. B. (2001). Changes in diet and
843 body condition of lake whitefish in southern Lake Michigan associated with changes in
844 benthos. *North American Journal of Fisheries Management*, *21*(4), 876-883.

845 Rao, Y. R., Hawley, N., Charlton, M. N., & Schertzer, W. M. (2008). Physical processes and
846 hypoxia in the central basin of Lake Erie. *Limnology and oceanography*, *53*(5), 2007-2020.

847 Rao, Y. R., & Murthy, C. R. (2001). Coastal boundary layer characteristics during summer
848 stratification in Lake Ontario. *Journal of Physical Oceanography*, *31*(4), 1088-1104.

849 Rao, Y. R., & Schwab, D. J. (2007). Transport and mixing between the coastal and offshore waters
850 in the Great Lakes: a review. *Journal of Great Lakes Research*, *33*(1), 202-218.

851 Schwab, D. J., & Rao, D. B. (1977). Gravitational oscillations of Lake Huron, Saginaw Bay,
852 Georgian Bay, and the North Channel. *Journal of Geophysical Research*, *82*(15), 2105-2116.

853 Schott, F., & Quadfasel, D. (1979). Lagrangian and Eulerian measurements of horizontal mixing
854 in the Baltic. *Tellus*, *31*(2), 138-144.

855 Sheng, J., & Rao, Y. R. (2006). Circulation and thermal structure in Lake Huron and Georgian
856 Bay: Application of a nested-grid hydrodynamic model. *Continental Shelf Research*, *26*(12-13),
857 1496-1518.

858 Sherman, R. K., Whittam, R., & Cayley, J. (2018). Severn Sound Remedial Action Plan: The
859 friendly little monster. *Aquatic Ecosystem Health and Management 21*(4), pp.387-397

860 Sly, P. G., & Munawar, M. (1988). Great Lake Manitoulin: Georgian Bay and the North Channel.
861 In *Limnology and Fisheries of Georgian Bay and the North Channel Ecosystems* (pp. 1-19).
862 Springer, Dordrecht.

863 Strayer, D. L., Hattala, K. A., & Kahnle, A. W. (2004). Effects of an invasive bivalve (Dreissenid
864 mussels polymorpha) on fish in the Hudson River estuary. *Canadian Journal of Fisheries and*
865 *Aquatic Sciences*, *61*(6), 924-941.

866 Suominen, T., Tolvanen, H., & Kalliola, R. (2010). Surface layer salinity gradients and flow
867 patterns in the archipelago coast of SW Finland, northern Baltic Sea. *Marine environmental*
868 *research*, *69*(4), 216-226.

869 Vanderploeg, H. A., Nalepa, T. F., Jude, D. J., Mills, E. L., Holeck, K. T., Liebig, J. R., ... &
870 Ojaveer, H. (2002). Dispersal and emerging ecological impacts of Ponto-Caspian species in the
871 Laurentian Great Lakes. *Canadian Journal of Fisheries and Aquatic Sciences*, *59*(7), 1209-1228.

872 Taylor, G. I. (1922). Diffusion by continuous movements. *Proceedings of the London*
873 *Mathematical Society*, *2*(1), 196-212.

874 Trebitz, A. S., Hatzenbuhler, C. L., Hoffman, J. C., Meredith, C. S., Peterson, G. S., Pilgrim, E.
875 M., ... & Wick, M. J. (2019). Dreissena veligers in western Lake Superior–Inference from new
876 low-density detection. *Journal of Great Lakes research*, *45*(3), 691-699.

877 Welch, P. (1967). The use of fast Fourier transform for the estimation of power spectra: a method
878 based on time averaging over short, modified periodograms. *IEEE Transactions on audio and*
879 *electroacoustics*, *15*(2), 70-73.

880 Whittier, T. R., Ringold, P. L., Herlihy, A. T., & Pierson, S. M. (2008). A calcium-based invasion
881 risk assessment for zebra and quagga mussels (Dreissena spp). *Frontiers in Ecology and the*
882 *Environment*, *6*(4), 180-184.

883 Zimmerman, J. F. T., & Kjerfve, B. (1988). Estuarine residence times. *Hydrodynamics of*
884 *estuaries, edited by: Kjerve, B*, *1*, 75-84.